Combined indocyanine green and quantitative perfusion assessment with hyperspectral imaging during colorectal resections: supplement

A. PFAHL,[1,5,*] G. K. RADMACHER,[2,5] H. KÖHLER,[1] M. MAKTABI,[1] T. NEUMUTH,[1] A. MELZER,[1,3] I. GOCKEL,[2] C. CHALOPIN,[1] AND B. JANSEN-WINKELN[2,4]

[1]*Innovation Center Computer Assisted Surgery (ICCAS), Faculty of Medicine, Leipzig University, Leipzig, 04103, Germany*

[2]*Department of Visceral, Thoracic, Transplant, and Vascular Surgery, University Hospital of Leipzig, Leipzig, 04103, Germany*

[3]*Institute for Medical Science and Technology (IMSaT), University of Dundee, Dundee, DD2 1FD, United Kingdom*

[4]*Department of General, Visceral, Thoracic, and Vascular Surgery, Klinikum St. Georg, Leipzig, 04129, Germany*

[5]*Contributed equally*

*annekatrin.pfahl@medizin.uni-leipzig.de

Combined Indocyanine Green and Quantitative Perfusion Assessment with Hyperspectral Imaging during Colorectal Resections: supplemental document

1. Spectral features

At the beginning of the study, twelve spectral features resulted from the spectral analysis of annotated hyperspectral data. These included mean, minimum, and maximum values of the reflectance spectrum $R(x,y,\lambda)$, its first or second derivative in specific spectral ranges as well as differences of these values. In some cases, the standard normal variate (SNV) [Eq.(S1)] with $R_{(x,y),SNV}(\lambda)$ as normalized reflectance spectrum of pixel (x,y), $R_{(x,y)}(\lambda)$ as raw reflectance spectrum, $\overline{R}_{(x,y)}$ as mean value along the spectral dimension λ, and $\sigma_{R(x,y)}$ as the standard deviation of this pixel along λ, served for normalization of reflectances to compensate spectral offsets due to environmental influences during the data acquisition. Furthermore, spectral features either originated from (a) the differential reflectance spectrum $R_{diff}(x,y,\lambda)$ (x,y,λ) of two hypercubes or (b) the reflectance spectrum of only one cube recorded after the ICG administration ($R_{post}(x,y,\lambda)$). For (a), one hypercube was recorded before ICG was given ($R_{pre}(x,y,\lambda)$) and was therefore unaffected by ICG. The second cube corresponded with the one that was used for (b) and comprised information on ICG. An overview of all twelve features can be found in Table S1.

For a quantitative comparison and the selection of the most promising spectral features for the ICG signal reconstruction from hyperspectral data, the calculated values over all included data sets were plotted against the ICG values, gathered from annotated ICG data. After a first-degree least-squares polynomial fit, the coefficient of determination r^2 with $r^2=1$ as the optimal solution was calculated. Here, the study population was divided regarding the given ICG dose. Thirty-six patients got 2.5 mg ICG (group 1) and 10 got 5 mg (group 2). Values for r^2 for each spectral feature as well as for both patient groups are listed in Table S1 as well.

Comparing all spectral features basing on (a), the differential spectrum, the difference of the maximum value from 810 to 830 nm and the minimum value from 770 to 790 nm of the first derivate of the non-normalized differential spectrum performed best over both groups ($r^2=0.15$ and $r^2=0.19$ for groups 1 and 2, respectively). This formed the basis for the difference method.

Features originating from R_{post} only, often led to values of r^2 smaller than 0.15 for group 1. However, for group 2, all features performed better than those using the differential reflectance spectrum. Here, the feature calculating the mean value in the spectral range from 790 to 810 nm of the second derivative of R_{post} stood out.

The described features that are the most appropriate ones for the ICG signal reconstruction are highlighted in Table S1.

$$R_{(x,y),SNV}(\lambda) = \frac{R_{(x,y)}(\lambda) - \overline{R}_{(x,y)}}{\sigma_{R_{(x,y)}}} \qquad (S1)$$

2. Influence of ICG on HSI parameter images

The influence of ICG on HSI data was assumed to be directly proportional to the volume of injected contrast agent and additionally, to be high directly after injection and to decrease over time. The scaled absolute mean differences for the HSI parameter images were considered as functions of the ICG bolus divided by the patient's body mass in mg/kg and of the time difference between the administration of ICG and the recording of the post-cube. The linearly

assumed dependencies of the differences of the oxygen saturation of tissue (StO_2), the near-infrared spectral range (NIR PI), the organ hemoglobin index (OHI), the tissue water index (TWI), and the tissue lipid index (TLI) are shown in Fig. S1.
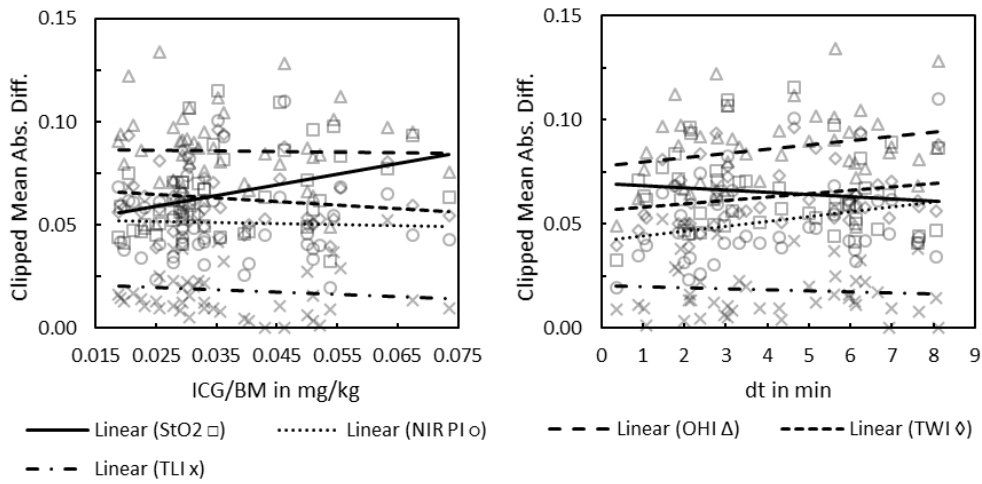

Fig. S1. Mean absolute differences between registered parameter images generated from hypercubes recorded both before and after ICG administration. Values are given as functions of the ICG dose in mg per kg body mass (left) and the time difference between ICG administration and post-cube acquisition in min (right).

Table S1. Calculation of spectral features from reflectance data R with $\dot{R} = dR/d\lambda$ and $\ddot{R} = d^2R/d\lambda^2$.

	Reflectance Data R	Value	Spectral Range in nm	SNV Norm.	r^2 (n=36, 2.5 mg ICG)	r^2 (n=10, 5 mg ICG)
1	$R_{post}(x,y,\lambda)$	$\mathrm{mean}(R)$	$\{\lambda \in \mathbb{Z} \mid 780 \leq \lambda \leq 820\}$	Yes	0.07	0.35
2	$R_{diff}(x,y,\lambda)$	$\min(R)$	$\{\lambda \in \mathbb{Z} \mid 790 \leq \lambda \leq 820\}$	Yes	0.08	0.16
3	$\dot{R}_{post}(x,y,\lambda)$	$\mathrm{mean}(R)$	$\{\lambda \in \mathbb{Z} \mid 760 \leq \lambda \leq 790\}$	Yes	0.09	0.31
4	$\dot{R}_{post}(x,y,\lambda)$	$\mathrm{mean}(R)$	$\{\lambda \in \mathbb{Z} \mid 810 \leq \lambda \leq 840\}$	Yes	0.08	0.25
5	$\dot{R}_{diff}(x,y,\lambda)$	$\min(R)$	$\{\lambda \in \mathbb{Z} \mid 770 \leq \lambda \leq 790\}$	No	0.11	0.14
6	$\dot{R}_{diff}(x,y,\lambda)$	$\max(R)$	$\{\lambda \in \mathbb{Z} \mid 810 \leq \lambda \leq 830\}$	No	0.05	0.19
7	$\dot{R}_{diff}(x,y,\lambda)$	$\min(R)$	$\{\lambda \in \mathbb{Z} \mid 770 \leq \lambda \leq 790\}$	Yes	0.10	0.12
8	$\dot{R}_{diff}(x,y,\lambda)$	$\max(R)$	$\{\lambda \in \mathbb{Z} \mid 810 \leq \lambda \leq 830\}$	Yes	0.07	0.16
9	$\dot{R}_{diff}(x,y,\lambda)$	$\max(R_{\lambda_1}) - \min(R_{\lambda_2})$	$\{\lambda_1 \in \mathbb{Z} \mid 810 \leq \lambda_1 \leq 830\}$ $\{\lambda_2 \in \mathbb{Z} \mid 770 \leq \lambda_2 \leq 790\}$	No	0.15	0.19
10	$\dot{R}_{diff}(x,y,\lambda)$	$\max(R_{\lambda_1}) - \min(R_{\lambda_2})$	$\{\lambda_1 \in \mathbb{Z} \mid 810 \leq \lambda_1 \leq 830\}$ $\{\lambda_2 \in \mathbb{Z} \mid 770 \leq \lambda_2 \leq 790\}$	Yes	0.17	0.15
11	$\ddot{R}_{post}(x,y,\lambda)$	$\mathrm{mean}(R)$	$\{\lambda \in \mathbb{Z} \mid 790 \leq \lambda \leq 810\}$	No	0.24	0.46
12	$\ddot{R}_{post}(x,y,\lambda)$	$\mathrm{mean}(R)$	$\{\lambda \in \mathbb{Z} \mid 790 \leq \lambda \leq 810\}$	Yes	0.24	0.44